Anal Bioanal Chem (2003) 377 : 1007–1013
DOI 10.1007/s00216-003-2191-8

PAPER IN FOREFRONT

Hai Miao · Stanislav S. Rubakhin · Jonathan V. Sweedler

Analysis of serotonin release from single neuron soma using capillary electrophoresis and laser-induced fluorescence with a pulsed deep-UV NeCu laser

Received: 3 June 2003 / Revised: 17 July 2003 / Accepted: 18 July 2003 / Published online: 9 October 2003

Abstract The use of capillary electrophoresis (CE) with laser-induced fluorescence excited by ultraviolet (UV) lasers in the range 200–300 nm has been restricted by the available wavelengths and expense of UV lasers. The integration of a NeCu deep UV laser operating at 248.6 nm with a single channel CE system with post-column sheath flow detection allows detection limits for serotonin and tryptophan of 3.9×10^{-8} M and 4.5×10^{-8} M respectively. Single cell analysis of serotonergic metacerebral cells from the sea slug *Aplysia californica* yields a value of 800±85 fmol of serotonin in each cell soma. For the first time, serotonin is directly detected in electrically stimulated release from single metacerebral cell soma, with approximately 4% of the serotonin contained in the soma released from a semi-intact preparation with a 2 min electrical stimulation.

Keywords NeCu laser · Capillary electrophoresis · Single cell analysis · Release · Serotonin

Introduction

Single cell analysis provides a wealth of information on the chemical environment within a cell. Studying the dynamic chemical changes occurring in single neurons, such as the release, metabolism and uptake of signaling molecules is a significant measurement challenge. Although neurotransmitter release occurs predominantly at synapses, several studies have examined transmitter secretion from neuronal soma. Somatic release of dopamine (DA) from mammals (rat substantia nigra and retinal neurons) and a pond snail (*Planorbis corneus*) has been observed using electrochemical methods [1, 2, 3]. Poo and coworkers detected the quantal release of acetylcholine (Ach) from *Xenopus* spinal neuron soma [4] and the evoked Ach secretion from the soma of dissociated hippocampal neurons [5]. Besides classical transmitters, Huang et al reported the Ca^{2+} dependent exocytosis of the neuropeptide substance P in the somata of dorsal root ganglion neurons [6]. Recently, the De-Miguel group indirectly observed the somatic release of serotonin (5-HT) from cultured Retzius neurons of the leech by the release of the fluorescent dye FM 1–43 during stimulation [7], which assumed the FM 1–43 was contained in the 5-HT vesicles and moved with the transmitters inside [8]. We demonstrate the direct measurement of 5-HT release from individual neuron somata under electrical stimulation using the metacerebral neuron of *Aplysia californica* as a model serotonergic neuron.

In order to obtain chemical, temporal and/or spatial information about trace levels of neurotransmitters released from a single neuron into the chemically-complex extracellular environment, sensitive and reliable analytical methods are required [9, 10]. Several techniques have been used to investigate the process of exocytosis, including intracellular fluorescent probes [11], membrane capacitance measurements [12], fluorescence microscopy based on an ultraviolet (UV) laser and a charge-coupled device detector [13, 14], mass spectrometry [15], capillary electrophoresis (CE) and capillary high performance liquid chromatography with laser-induced fluorescence (LIF) [16, 17, 18, 19] and electrochemical detection [20, 21, 22, 23]. CE is an ideal tool for trace-level transmitter analysis because of its rapid separation ability, high separation efficiency, small sample consumption and compatibility with biological environments [24]. Despite the fact that LIF detection of derivatized analytes provides excellent limits of detection (LODs) for CE [25, 25, 26, 27], limitations in the chemistry [13] can cause incomplete reactions, especially when the analyte concentration is low, which is the case in single cell analysis. Laser-induced native fluorescence (LINF) detection is an alternative to fluorescent derivatization for compounds that are natively fluorescent. Yeung's research group has done pioneering research using CE with LINF detection of analytes applied to single cell studies using the 275 nm line from a large frame continuous wavelength (CW) Ar ion laser for excitation. Based

H. Miao · S. S. Rubakhin · J. V. Sweedler (✉)
Department of Chemistry and the Beckman Institute,
University of Illinois, Urbana, 61801, USA
e-mail: sweedler@scs.uiuc.edu

on hydrodynamic injection and on-column detection, they explored the release of 5-HT from single rat peritoneal mast cells [17, 28], norepinephrine and epinephrine from individual bovine adrenal chromaffin cells [18], and insulin from insulin-secreting βTC3 cells [19]. 5-HT depletion from both neurons and neuroglia has also been monitored using LINF imaging, which displays both temporal and spatial resolution [14, 29]. We have used CE with LINF to characterize the contents of neurons and discovered novel 5-HT catabolites using wavelength-resolved native fluorescence detection [30, 31, 32, 33].

Since the early 1990s, improvements in pulsed UV lasers have emerged and provided advantages for such systems. Gooijer's research group has undertaken a systematic study of pulsed laser performance, including the XeCl excimer lasers, the frequency-quadrupled Nd:YAG lasers, and the nitrogen laser. These lasers were compared to the conventional CW UV laser [34, 35]. They also demonstrated that the 280 nm laser line from a pulsed excimer-dye laser was more suitable to analyze substituted naphthalene sulphonates in river water than the 257 nm line from a frequency-doubled CW Ar ion laser, because of the interference with shorter excitation wavelength [36]. The Issaq group successfully separated tryptophan and ten related indoles under 17 min and obtained nanomolar concentration LODs using micellar electrokinetic chromatography with LINF excited by a pulsed KrF excimer laser (λ=248 nm) [37]. Paquette and coworkers applied this laser to investigate the profile of human urine, saliva and serum and obtained a LOD of 7–170 nM for indole-based compounds and catecholamine urinary metabolites [38].

Although LINF detection has many advantages when performing mass-limited sample analysis, it has not become common because of the expense and complexity of many of these UV lasers [30]. We demonstrate here the use of a relatively inexpensive NeCu deep-UV laser (~US$10,000 with an expected life expectancy of ~1 year and tube replacement cost of <US$4,000, while a 248 nm KrF excimer laser costs about $30,000 [39]). We interface this laser to a conventional single channel CE system with photomultiplier tube (PMT) detection. The LOD of 40 nM is comparable or better than systems using 248 nm pulsed UV lasers, allowing the detection of 5-HT release from single electrically stimulated metacerebral cell (MCC) soma.

Materials and methods

Reagents

The borate running buffer (50 mM, pH 8.5) was prepared using 3.0 g of boric acid (H_3BO_3; Sigma, St. Louis, Mo.), and 9.2 g of sodium borate ($Na_2B_4O_7{\cdot}10H_2O$; Sigma) in 1.00 L of ultrapure de-ionized water (Milli-Q filtration system; Millipore, Belford, Mass.). The sheath flow buffer was of the same composition as the running buffer. All standards were obtained from Sigma and were reagent quality or better. Standard solutions were made with Milli-Q water and filtered with 0.45 µm acrodisc syringe filter (Gelman Laboratory, Ann Arbor, Mich.).

Instrumentation

Fig. 1 is a schematic diagram of the assembled CE system with LINF detection. A 50-µm i.d., 350-µm o.d. untreated, fused silica capillary (Polymicro, Phoenix, Ariz.) was employed for separation. The capillary length for standards separation and single cell cytoplasm analysis was 68 cm and the capillary length for release study was 62 cm. At both ends, a 5-mm long section of the polyimide coating was removed. A homebuilt nanovial injection system appropriate for cell measurements and cellular release injection, similar to what previously described [15], was used for electrokinetic sample injections. A stainless steel cylindrical block controlled by a rotary stage (Model RSA-2T, Newport) was connected to the positive end of a high voltage power supply (High Bridge, N.J.) as the anode. Microvials and nanovials containing separation buffer and sample solution were placed in the drilled holes in the stainless steel block, and the injection platform was held in an acrylic box with safety interlocks. As the microvial and nanovial were also made of stainless steel, high voltage applied to the cylindrical block was applied to the sample and separation buffer in the vials.

For the cellular assays, rinsing steps were required to prevent protein build-up on the capillary walls. Between each separation, the capillary was rinsed, using a 1 mL syringe (Becton Dickinson, Franklin Lakes, N.J.), with 0.2 M NaOH for 1 min, Milli-Q water for 2 min, and the running buffer for 2 min, and equilibrated for at least 5 min under separation conditions. The electrokinetic injection time was 2 s at 5 kV and the separation voltage was 25 kV. Under these conditions, the capillary current was approximately 30 µA at 25 kV and the injection current was around 5 µA at 5 kV.

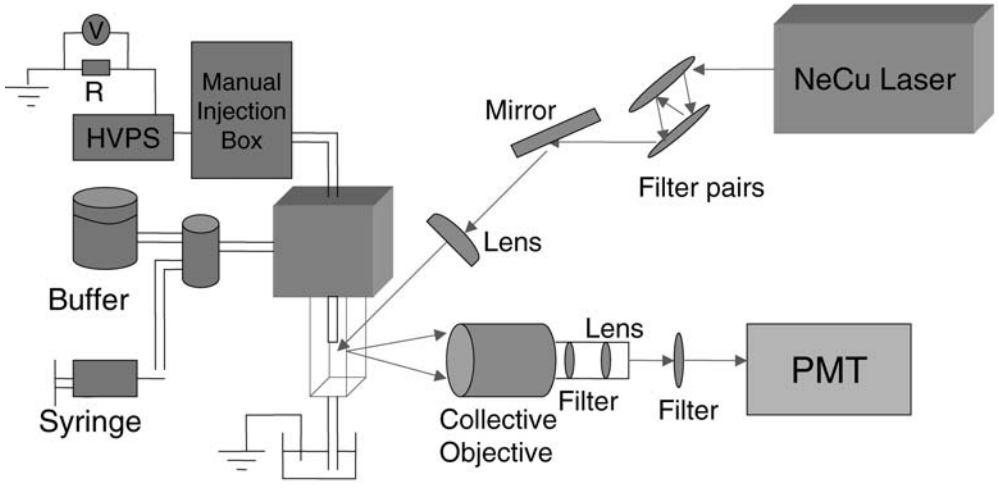

Fig. 1 Schematic diagram of the custom capillary electrophoresis-laser-induced native fluorescence system with a NeCu laser as excitation light source and a sheath-flow assembly as the detection cell. *HVPS* High-voltage power supply, *PMT* photomultiplier tube

A post-column sheath flow assembly was used to improve the LOD by eliminating the scattered light from the capillary [40, 41]. In general, the LOD of post-column sheath flow detection is more than an order of magnitude lower than that of traditional online detection [42], and Dovichi's group has reported a LOD of as low as ~6 molecules for sulforhodamine 101 using sheath flow detection [43]. When using UV excitation, the broad capillary luminescence background is especially problematic, necessitating a sheath flow system. The capillary outlet was centered in a 1×1×20 mm quartz cuvette (NSG precision cells, Farmingdale, N.Y.) serving as the sheath flow chamber. The sheath flow was driven by the height difference between the liquid levels of the sheath flow reservoir and the waste reservoir, and the linear sheath flow speed was approximately 1 mm/s. A T-shape valve was used to switch between the normal sheath flow and the flow to rinse the cuvette.

The 248.6 nm UV laser (Photon systems, Covina, Calif.) was introduced at ~10° to the normal and reflected four times by two reflective edge filters (250 nm long pass) facing each other at a distance of about 4 cm. The parallel filters eliminated or suppressed the tube plasma glow from the NeCu laser. After reflection by an UV mirror, the laser was focused to the outlet of the capillary in a sheath flow assembly by a silica focusing-lens (Linos 312256, Milford, Mass.). The collection arm was orthogonal to the excitation arm and the fluorescence was collected with a 15× all-reflective microscope objective (ThermoOriel, catolog #13595,Stratford, Conn.). After passing through a UV filter (EO, UG360, Barrington, N.J.), a focusing lens and a spatial filter, the appropriate fluorescence signal was monitored by a PMT module (HC-135–01, Hamamatsu, Middlesex, N.J.). A National Instrument data acquisition board (AT-MIO-16F-5) and an in-lab-written Labview program were used to coordinate the communication between the CPU, the PMT and the nanoinjector.

Animal and cell preparation

A. californica (100–200 g) were obtained from Aplysia Research Facility (University of Miami, Miami, Fl.) and kept in an aquarium containing continuously circulating, aerated and filtered artificial sea water (ASW) at 14–15 °C until used. Animals were anesthetized by injection of isotonic $MgCl_2$ (~30–50% of body weight) into the body cavity. The cerebral ganglia were dissected and placed in normal ASW containing 460 mM NaCl, 10 mM KCl, 10 mM $CaCl_2$, 22 mM $MgCl_2$, 6 mM $MgSO_4$, and 10 mM HEPES, pH 7.7 or in ASW-antibiotic solution (normal ASW supplied with 100 units/mL penicillin G, 100 µg/mL streptomycin, and 100 µg/mL gentamicin, pH 7.7). The ganglionic sheath was digested enzymatically by incubating the ganglia in ASW-antibiotic solution containing 1% protease (type IX: bacterial; Sigma) at 36 °C for 1–2 h depending on animal size. Next, the ganglia were washed in fresh ASW. Using 0.38-mm diameter tungsten wire (WPI, Sarasota, Fl.), the ganglia were pinned dorsal side up to a silicone elastomer (Sylgard, Dow Corning, Midland, Mich.) layer in a recording chamber filled with 3–4 mL of ASW-antibiotic media. The dorsal side of the cerebral ganglia was mechanically desheathed. The isolated ganglia preparation was incubated in ASW-antibiotic solution at 14 °C for at least 1 h before each experiment.

Electrophysiology

Glass microelectrodes (8–15 MΩ) pulled from 1 mm borosilicate glass capillaries (WPI) and filled with 506.2 mM KCl, 5 mM HEPES solution (pH 7.6) were used for intracellular recording and stimulation of MCC neurons. Signals were amplified with an Axon (Union City, Calif.) AxoClamp 2B amplifier, monitored and stored with a PC computer using a Digidata 1322A D/A-A/D converter (Axon). The software package pClamp 8 (Axon) was used for data acquisition and analysis. Records were digitized at 2–10 kHz and filtered with a low-pass Bessel filter at 10-kHz cutoff frequency. All experiments were performed at room temperature (22–24 °C).

Stimulation and collection of serotonin release

Release from MCC neuronal soma was collected continuously through a 350 µm i.d. fused silica capillary (Polymicro) micropositioned to within 0.5–1.5 mm from cell surface. Fast green (5 mg/mL) was used for visual adjustment of this release collection system. Action potentials were stimulated for 2 min in normally silent MCCs by current injection (160 ms 1–5 nA square pulses, 520 ms interpulse interval). Control samples were collected before and after neuron stimulation. Every sample contained cellular release accumulated for 2 min.

Fluorometry

The excitation spectra measurements were performed with a spectrofluorometer (F-3010, Hitachi, Tokyo, Japan). The scan range of the excitation wavelengths was 200–320 nm and the emission wavelength was set at 340 nm with a bandwidth of 10 nm. Scan rate and response time were 60 nm/min and 2 s, respectively. The fluorescence spectra data were processed with Microsoft Excel software.

Results and discussion

System characterization and optimization

Figure 1 shows the schematic diagram of the CE-LIF system with the NeCu laser as the excitation source. This laser, like many gas lasers, produces a significant background excitation that must be removed or the background is too high for fluorescence measurements. A parallel edge filter pair is used to remove the tube glow and incoherent emission interference [30]. The circular laser spot is ~3 mm in diameter and the laser is designed for multimode operation. Assuming a Gaussian beam profile and using a 1.5-cm focal length (f.l.) lens, the expected spot size is ~1.2 µm in diameter, and is 4 µm for a 5-cm f.l. lens, both significantly smaller than the expected sheath lumen diameter. We have compared the performance of two focusing lenses with focal lengths of 1.5 cm and 5.0 cm respectively. The peak intensity obtained with the 1.5 cm lens was about three times higher than that of the 5.0 cm lens and the spot appeared more homogeneous. Thus, the 1.5 cm f.l. lens was used in all further experiments.

Unlike many pulsed lasers that have low duty cycles (10^{-5}–10^{-6}) [35, 36], the NeCu laser has a duty cycle of ~3.3×10^{-3} at the default setting (30 µs, 110 Hz). A low repetition rate results in fewer data points across the peak, and a low duty cycle results in poorer performance [44]. The microsecond pulse width and the several-hundred hertz repetition rate allow the pulsed laser to be used as a pseudo-continuous wave laser, simplifying its use for CE-LIF. The high duty cycle also indicates that for a given average power, the peak power is low enough to reduce saturation and photobleaching effects. The average output power of the NeCu laser obviously depends on the repetition rate, and the tube lifetime is inversely proportional to repetition rate; the average power is ~0.54 mW at the 110 Hz frequency, 0.73 mW at 150 Hz and 0.90 mW at 200 Hz, all with a 30 µs pulse width and 25 A drive current. The power is measured after the parallel filter pair and before the reflecting mirror.

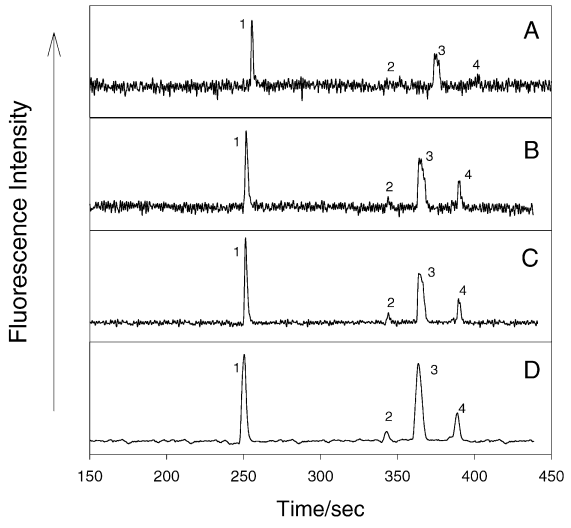

Fig. 2A–D Fluorescent intensity of standards obtained at different NeCu laser operating parameters (driving current, pulse frequency) and data process methods. (**A**) 25A, 110 Hz; (**B**) 50A, 110 Hz; (**C**) 50A, 192 Hz; (**D**) 50A, 192 Hz, with six-point boxcar average data processing. *1* Serotonin (5-HT), *2* DA, *3* tryptophan (Trp), *4* tyrosine (Tyr)

Figure 2 shows the electropherograms of 1.2×10^{-6} M 5-HT and Trp, and 2.5×10^{-5} M DA and Tyr standards obtained using different laser parameters and data processing methods. The S/N of all standards increased with increasing tube driving current and pulse frequency. When the laser was operated at 25 A and 110 Hz, DA was difficult to detect and the Tyr peak had a low intensity. The detection performance for Tyr and DA greatly improved when the driving current was increased to 50 A, and the frequency to 192 Hz. Thus, the higher operating frequency and the laser power markedly aid the system performance for these analytes.

Usually the LOD for LINF is limited by the noise in the background. Boxcar averaging not only decreases high frequency fluctuations but also reduces electrophoretic resolution. Interestingly, the S/N ratio increased by a factor of ~2.3 after averaging six consecutive points with this laser (Fig. 2), while an increase of only ~1.1 was observed using a 457 nm CW Ar-ion laser (data not shown), with the same 2 Hz acquisition rate used for both experiments. This produces a decrease of ~35% in separation efficiency. We use this data processing method when LODs are important and when the decrease in separation efficiency of 35% is not critical. With native fluorescence detection and 248 nm excitation, few compounds fluoresce, and so the resolution reduction is often an acceptable tradeoff, as opposed to approaches using chemical derivatization of amine groups, resulting in more complex electropherograms requiring higher separation efficiency to resolve all components. Table 1 shows the LODs of the four standards. The calibration curve for 5-HT under the default setting is $y=0.8884x+8.2127$ with $R^2=0.997$ (data not shown), where y is the logarithm of fluorescent intensity and x is the logarithm of 5-HT concentration. The linear range is from ~2×10^{-7} M to ~5×10^{-4} M, and the calibration curve levels off at ~10^{-3} M, likely because of self-quenching [29]. Increased performance for many analytes can be achieved at higher repetition rates at the cost of tube lifetime. A dynamic approach of increasing the repetition rate only during the periods corresponding to the expected elution of specific analytes may offer the greatest tradeoffs between performance and laser lifetime.

Table 1 LODs obtained at different NeCu laser settings

	5-HT (M)	Trp (M)	Tyr (M)	DA (M)
25 A, 110 Hz	2.9×10^{-7}	4.2×10^{-7}	2.1×10^{-5}	4.8×10^{-5}
25 A, 110 Hz[a]	1.0×10^{-7}	1.5×10^{-7}	8.0×10^{-6}	2.4×10^{-5}
50 A, 110 Hz	1.5×10^{-7}	2.4×10^{-7}	1.0×10^{-5}	2.5×10^{-5}
50 A, 110 Hz[a]	7.0×10^{-8}	9.0×10^{-8}	4.3×10^{-6}	1.3×10^{-5}
50 A, 192 Hz	7.0×10^{-8}	1.2×10^{-7}	4.7×10^{-6}	1.1×10^{-5}
50 A, 192 Hz[a]	3.9×10^{-8}	4.5×10^{-8}	2.3×10^{-6}	6.0×10^{-6}

[a]With 6-point boxcar averaging

Single cell analysis

The MCC neuron is an important serotonergic neuron in the feeding networks of opisthobranch mollusks, and numerous studies have explored its biochemistry, physiology and neurochemistry [32, 45, 46, 47]. After the MCC neuron was manually isolated from the cerebral ganglion and transferred to a nanovial, borate buffer was added to the vial where lysis of the cell occurs. The final volume of the sample was ~300 nL. The NeCu laser was operated at 25 A, 30 µs and 110 Hz here, as the sensitivity is adequate for whole cell 5-HT analysis. Figure 3 is a typical electropherogram from a single MCC neuron injection. 5-HT, Trp and Tyr were detected with good S/N ratio. The peak shoulders at ~350 s are from neutral cellular compounds. The broad peaks between 500 and 700 s are from unresolved proteins that contain Tyr and Trp [31]. Analytes

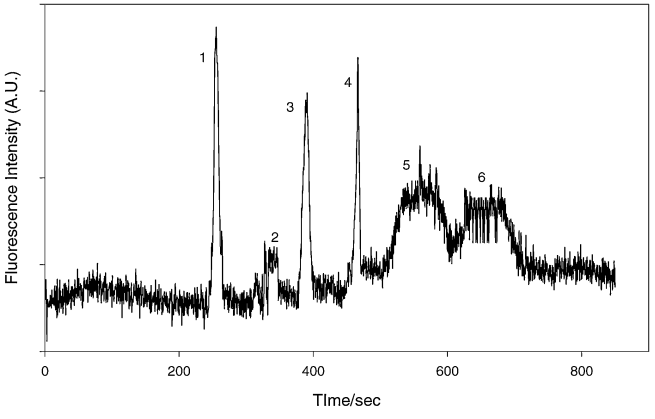

Fig. 3 Electropherogram of a single metacerebral cell (MCC) neuron from *Aplysia californica* showing 5-HT, Trp, Tyr and an unresolved protein band. *1* 5-HT, *2* EOF and/or neutral compounds, *3* Trp, *4* Tyr, *5* and *6* unresolved proteins

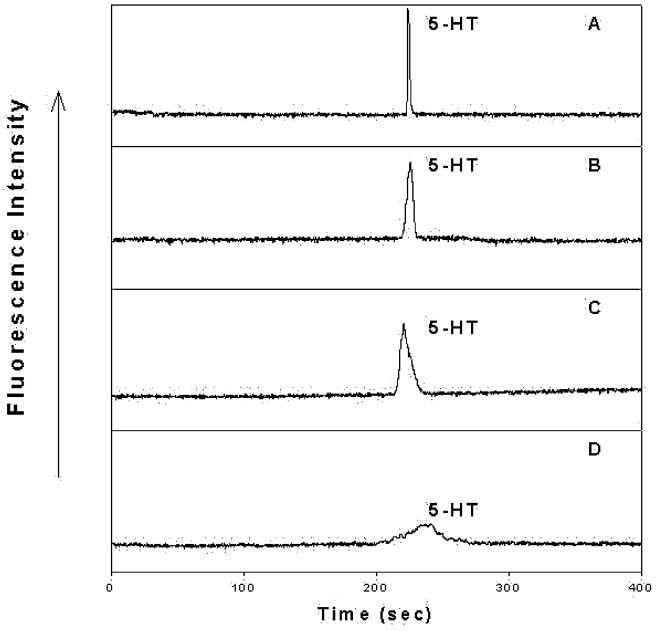

Fig. 4A–D Electropherograms of *5-HT* dissolved in solutions with different ratios of 50 mM borate buffer and artificial seawater (ASW)(v/v). **A** Borate buffer 50 mM. **B** Buffer to seawater 1:4. **C** Buffer to seawater 1:1. **D** ASW

such as 5-HT, Trp and Tyr had 5%, 8% and 8% temporal reproducibility (reproducibility was calculated as $(T_{max}$-$T_{min})/T_{ave}\times100\%$, where T_{max}, T_{min} and T_{ave} stand for maximum, minimum and average migration times) from cell injection to cell injection (n=6). The 5-HT amount detected in each MCC was 800±85 fmol. Estimating the size of each MCC cell as 250±20 µm, the volume was ~8.2±2.0 nL, yielding a 5-HT concentration of 98±26 µM. The peak identities were confirmed by both migration time and spiking with standards. These experimental results agree well with our previous analysis of individual MCC neurons with a wavelength-resolved CE LINF system [31].

Single cell release detection

Measuring the electrically-evoked release from a cell is more difficult than assaying the cellular contents. Obviously, only a small fraction of the neurotransmitter content from a neuron is released under chemical or electrical stimulation and this is rapidly diluted into the media surrounding the cell. In order to keep the *A. californica* MCC neuron alive, media at the ionic strength of seawater must surround the neuron during entire experiment. Although CE has the ability to separate analytes in high inorganic salt solutions, injecting 0.5 M inorganic salt solution into the electrolyte in the column reduces the separation efficiency.

Does the salt content influence the detection of 5-HT? The peak height of 2.5×10^{-6} M 5-HT dissolved in ASW was only about 20% of height when dissolved in 50 mM borate buffer, and the peak shape was distorted, usually due to fronting (Fig. 4). When the 5-HT solution was made in 1:1 (v:v) ASW:50 mM borate buffer, the 5-HT peak intensity was about 70% of the peak amplitude with 5-HT in 50 mM borate buffer. A further dilution of the solution to 1:4 (v:v) ASW:borate buffer resulted in a small increase in the 5-HT peak height and limited improvements in peak shape. The migration time, bandwidth, peak height and separation efficiency of 5-HT peaks under different sample solutions are listed in Table 2. Based on these results, release samples containing ~200 nL ASW were diluted with 200 nL borate running buffer before injection because the benefit of lowering the salt content outweighed the dilution of 5-HT.

Figure 5 shows a typical electropherogram of a MCC neuron release experiment. The NeCu laser was operated at 195 Hz pulse frequency and 50 A drive current for maximum sensitivity. No 5-HT was observed before or after the electrical stimulation, while 5-HT was consistently detected in samples collected near the electrically stimulated MCC neurons (n=6). The average 5-HT released for the 2 min stimulation pulse train was approximately 4% of the 5-HT stored in the MCC single neuron. Tyr, Trp and proteins were not detected, either because there is no release of these substances under electrical stimulation or the amount released is below the detection limit. To the best of our knowledge, this is the first demonstration of the detection of serotonin released from single soma in a semi-intact cell preparation measured using CE-LINF.

It is generally believed that the 5-HT vesicles are synthesized in the soma, and transported to the neuronal terminal, where the contents are released and the vesicles recycled. The participation of the soma in Ca^{2+} regulated exocytosis has not been well studied. Previously, DA, Ach and neuropeptide release have been measured from the neuronal cell body [1, 2, 3, 4, 5, 6]. Our result showing 5-HT released from the *Aplysia* MCC neuronal soma helps to generalize somatic secretion. A number of functions can be proposed for 5-HT released from MCC soma in vivo, including regulation of MCC activity through 5-HT autoreceptors or a paracrine action on locations in close

Table 2 5-HT peak characteristics under different sample buffers

	50 mM Borate buffer	1:4 (ASW:50 mM borate buffer v:v)	1:1 (ASW:50 mM borate buffer v:v)	ASW
Migration time (s)	224	222	226	~236 (broad)
Relative peak intensity	1	0.74	0.70	0.20
Band width (s)	1.6	5.6	9.0	35
Peak efficiency	110,000	8,700	3,500	250

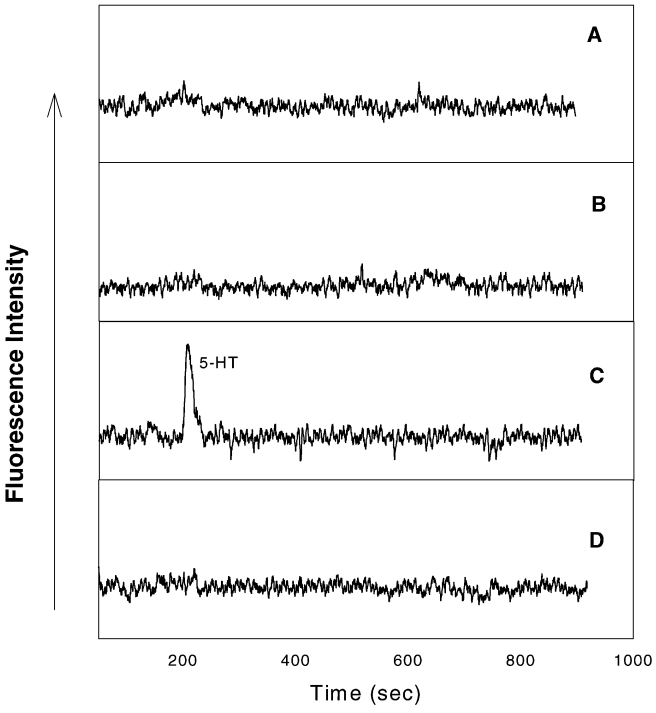

Fig. 5A–D Electropherograms of a single *A. californica* MCC soma release. Releasates collected for 2 min: (**A**) 4 min prior to stimulation, (**B**) 2 min before stimulatio, (**C**) during the 2-min electrical stimulation (**D**) and 4 min after stimulation. Electrical stimulation consisted of 160 ms, 1–5 nA square pulses, 520 ms interpulse interval (see text for further details). A six-point boxcar data averaging was used on the laser-induced fluorescence output

proximity to the MCC soma including glial cells, neurons, and elements of the ganglionic sheath. Hemolymph flow may transport this 5-HT pool to more distant targets. Interestingly, Zerby et al. reported that the sites of exocytotic events changed with the differentiation status of PC12 neurons [48], and Zheng et al. showed evidence that released transmitter acted as a trophic agent to guide the turning of neuronal growth cones [49]. Thus, somatic release is an area requiring further study.

Regarding the detection system, the 248.6 nm is not an optimum excitation wavelength for 5-HT analysis, as 248.6 nm is close to an absorbance minimum for 5-HT, Trp, Tyr and DA [30]. Fortunately, there are other possible laser lines using similar metal vapor lasers, such as 252.9 nm, 259 nm and 272 nm [39]. We previously demonstrated that the LOD obtained with 284 nm excitation for Trp and Tyr is more than 100 times lower than of 257 nm using a similar sheath flow system [50]. Lee et al. showed that the LOD of Trp- or Tyr-containing proteins decreased by two orders of magnitude with the excitation of 275 nm laser line compared to the 257 nm excitation [51]. Thus we expect that the 272 nm laser line for the metal vapor lasers will improve the LODs of these compounds by more than an order of magnitude in comparison to the 248.6 nm line, assuming similar quantum efficiency and photodegradation at these two wavelengths. Future work will also explore dynamically shifting the operating parameters of the laser, so that the highest sensitivity is obtained for specific analytes with other sections in the electropherograms having lower laser power output.

Acknowledgements This work was supported by the National Science Foundation (CHE-98–77071) and NIH (MH60261). The authors appreciate the advice and assistance of William Hug and Ray Raid (Photon System Inc.) concerning the operation of the NeCu laser, Xin Zhang (UIUC) for advice on 5-HT measurements, and Sarah Sheeley (UIUC) for assistance with construction of the CE system. *A. californica* were provided by the NCRR National Resource for Aplysia at the University of Miami.

References

1. Jaffe EH, Marty A, Schulte A, Chow RH (1998) J Neurosci 18:3548–3553
2. Puopolo M, Hochstetler SE, Gustincich S, Wightman RM, Raviola E (2001) Neuron 30:211–225
3. Chen G, Gavin PF, Luo G, Ewing AG (1995) J Neurosci 15: 7747–7755
4. Sun Y, Poo MM (1987) Proc Natl Acad Sci USA 84:2540–2544
5. Dan Y, Song HJ, Poo MM (1994) Neuron 13:909–917
6. Huang LM, Neher E (1996) Neuron17:135–145
7. Trueta C, Mendez B, De-Miguel FF (2003) J Physiol 547: 405–416
8. Betz WJ, Bewick GS, Ridg RM (1992) Neuron 9:805–813
9. Travis ER, Wightman RM (1998) Annu Rev Biophys Biomol Struct 27:77–103
10. Dahlgren R, Page JS, Sweedler JV (1999) Anal Chim Acta 400:13–26
11. Benz WJ, Mao F, Smith CB (1996) Curr Opin Neurobiol 6:365–371
12. Metthews G (1996) Curr Opin Neurobiol 6:358–365
13. Yeung ES (1999) Anal Chem 522A-529A
14. Tan W, Haydon PG, Yeung ES (1997) Applied Spectrosc 51:1139–1143
15. Rubakhin SS, Page JS, Monroe BR, Sweedler JV (2001) Electrophoresis 22:3752–3758
16. Phillips TM (2001) Luminescence 16:145–152
17. Ho AM, Yeung ES (1998) J Chromatogr A 817:377–382
18. Tong W, Yeung ES (1997) J Neurosci Methods 76:193–201
19. Tong W, Yeung ES (1997) J Chromatogr B 689:321–325
20. Miles PR, Mundorf ML, Wightman RM (2002) Synapse 44: 188–197
21. Bruns D, Jahn R (1995) Nature 377:62–65
22. Finnegan JM, Wightman RM (1995) J Biol Chem 270:5353–5359
23. Anderson BB, Ewing AG (1999) J Pharm Biomed Anal 12: 15–32
24. Stuart J, Sweedler JV (2003) Anal Bioanal Chem 375:28–29
25. Zhou SY, Zuo H, Stobaugh JF, Lunte CE, Lunte SM (1995) Anal Chem 67:594–599
26. Rocher C, Bert L, Robert F, Trouvin JH, Renaud B, Jacquot C, Gardier AM (1996) Brain Res 737:221–230
27. Liu YM, Sweedler JV (1995) Anal Chem 67:3421–3426
28. Lillard SJ, Yeung ES, McCloskey MA (1996) Anal Chem 68: 2897–2904
29. Parpura V, Tong W, Yeung ES, Haydon PG (1998) J Neurosci Methods 82:151–158
30. Zhang X, Sweedler JV (2001) Anal Chem 73:5620–5624
31. Fuller RR, Moroz LL, Gillette R, Sweedler JV (1998) Neuron 20:173–181
32. Zhang X, Stuart J, Sweedler JV (2002) Anal Bioanal Chem 376:332–343
33. Stuart JN, Zhang X, Jakubowski JA, Romanova EV, Sweedler JV (2003) J Neurochem 84:1358–1366
34. Van de Nesse RJ, Velthorst NH, Brinkman UAT, Gooijer C (1995) J Chromatogr A 704:1–25

35. Gooijer C, Kok SJ, Ariese F (2000) Analusis 28:679–685
36. Kok SJ, Isberg ICK, Gooijer C, Brinkman UAT, Velthorst NH (1998) Anal Chim Acta 360:109–118
37. Chan KC, Muschik GM, Issaq HJ (1995) J Chromatogr A 718:203–210
38. Paquette DM, Sing R, Banks PR, Waldron KC (1998) J Chromatogr B 714:47–57
39. Photonsystem http://www.photonsystems.com/products/laser.html
40. Oldenburg KE, Xi X, Sweedler JV (1997) Analyst 122:1581–1585
41. Timperman AT, Khatib K, Sweedler JV (1995) Anal Chem 67:139–144
42. Bowser MT, Kennedy KT (2001) Electrophoresis 22:3668–3676
43. Chen DY, Adelhelm K, Cheng XL, Dovichi NJ (1994) Analyst 119:349–352
44. Mank AJG, Velthorst NH, Brinkman UAT, Gooijer CJ (1995) Chromatogr A 695:175–183
45. Kim WS, Dahlgren RL, Moroz LL, Sweedler JV (2002) Anal Chem 74:5614–5620
46. Horn CC, Geizhals CR, Kupfermann I (2001) Brain Res 918:51–59
47. Koh HY, Jacklet JW (1999) J Neurosci 19:3818–3826
48. Zerby SE, Ewing AG (1996) Brain Res 712:1–10
49. Zhang JQ, Felder M, Connor JA, Poo MM (1994) Nature 368:140–144
50. Timperman AT, Oldensburg KE, Sweedler JV (1995) Anal Chem 67:3421–3426
51. Lee TT, Yeung ES (1992) J Chromatogr A 595:319–325